Journal of Applied Polymer Science

Characterization of MAO-Modified Silicas for Ethylene Polymerization

Mohamad Mehdi Mortazavi,[1] Saeid Ahmadjo,[1] Joao Henrique Zimnoch Dos Santos,[2] Hassan Arabi,[1] Mehdi Nekoomanesh,[1] Gholam Hossein Zohuri,[3] Rodrigo Brambilla,[2] Griselda Barrera Galland[2]

[1]Department of Catalyst, Iran Polymer and Petrochemical Institute, Tehran, Iran

[2] Department of Inorganic Chemistry, Instituto de Química, UFRGS, Av. Bento Gonçalves, 9500, Porto Alegre, 91501-970, Brazil

[3]Department of Chemistry, Faculty of Science, Ferdowsi University of Mashhad, Mashhad, Iran

Correspondence to: S. Ahmadjo (E-mail: s.ahmadjo@ippi.ac.ir)

ABSTRACT: A series of methylaluminoxane (MAO)-modified PQ and EP 12 silicas, calcined at 110, 250, and 450°C, were prepared. The resulting MAO-modified supports were characterized by a set of complementary techniques: Fourier transform infrared spectroscopy (FT-IR), scanning electron microscopy-energy dispersive X-ray spectroscopy (SEM-EDX), small angle X-ray scattering (SAXS), and thermal gravimetric analysis (TGA). The Al/Si ratios of the MAO-modified PQ and EP12 silicas were in the ranges of 0.19–0.27 wt % and 0.17–0.30 wt %, respectively. MAO-modified silicas were used in the polymerization of ethylene using an $Et_2IndZrCl_2$ catalyst. The MAO-modified PQ silica showed higher activity in comparison to the MAO-modified EP12. © 2013 Wiley Periodicals, Inc. J. Appl. Polym. Sci. 130: 4568–4575, 2013

KEYWORDS: polyolefins; grafting; catalysts

Received 2 May 2013; accepted 4 July 2013; Published online 27 July 2013
DOI: 10.1002/app.39737

INTRODUCTION

Single site metallocene catalysts have attracted much attention as they enable the production of polymers with narrow molecular weight distributions, uniform chemical compositions, and often high degrees of stereo-specificity.[1] Unfortunately, homogeneous metallocenes require large amounts of expensive MAO to exhibit maximum catalyst activities. This limitation may impair their commercial application to some extent. Therefore, much effort has been invested in decreasing the amount of MAO needed for efficient polymerization and finding new co-catalysts to replace it. Metallocene catalysts must be supported because homogeneous catalysts are unsuitable for gas phase and slurry processes.[2–5] Solution polymerization processes require the separation of the polymer from the solvent and the subsequent recovery and purification of the solvent. However, gas phase processes have lower costs and energy consumption. Several silica-supported metallocene catalyst systems have been reported in the literature.[3–7] They can be grouped into two main families: (i) those involving MAO mediated systems,[8,9] in which the surface of silica is modified with MAO prior to metallocene impregnation, and (ii) systems with metallocenes directly supported on carriers.[10] Research into metallocene heterogenization indicates that the physical impregnation of the catalyst or the physical grinding of the catalytic species with supports such as silica does not give rise to practical catalyst systems. This is due to a drastic reduction in the catalyst activity that is mainly attributed to low quantities of the immobilized metallocene.[11,12] Most of the studies employing chemically modified silicas focus on improving the access of monomer units to catalytically active sites through the use of spacers between the silica surface and the metallocene species. As judged from their reported catalytic activities, many of these studies have been quite successful.[3,13] Chu et al. proposed an alternative methodology (in situ supporting) using methylaluminoxane supported on silica (SMAO), a commercially available immobilized co-catalyst.[14,15] This approach consists of the direct addition of a catalyst solution to MAO supported silica inside the reactor immediately before pressurizing with a monomer. A review of the literature showed that studies investigating the influence of the properties of MAO-modified silica on the performance of the metallocene catalysts are fairly limited.

In the present article, the influence of the physical characteristics of the silica and the calcination temperature were investigated. Two commercial silicas were employed: PQ MS 3065 (PQ Corporation) and EP12 (Crossfield). The former is a silica gel with a very high pore volume, large surface area, and superior morphology; the latter is silica gel produced by the reaction of a mineral acid and sodium silicate exhibiting medium pore volume and surface area. The MAO-modified silicas were characterized by a set of complementary techniques in an effort to extract the relationships between the structural and textural characteristics of the support and the catalyst activity in the polymerization of ethylene.

EXPERIMENTAL

Material

Silicas EP12 and PQ MS 3065 were donated by Crossfield and PQ Incorporation and were calcinated under vacuum ($P < 10^{-4}$ mbar) for 6 h at the following temperatures: 110, 250, and 450°C. The support was cooled to room temperature under a dynamic vacuum and stored under dried argon. The MAO was supplied by Witco (7.0 wt % in a toluene solution), and the metallocene catalyst ($EtInd_2ZrCl_2$) was purchased from Aldrich. Ethylene and argon (White Martins) were passed through molecular sieves prior to use. Pure grade toluene was deoxygenated and dried using standard techniques.

MAO-Modified Silica Preparation

All experiments were performed under argon using proper Schlenk techniques. The MAO-modified silicas were prepared by grafting MAO on calcinated silica (ca., 1 g) using an MAO solution corresponding to 12 wt % of Al/SiO_2. The slurry was stirred for 2 h at room temperature. Thereafter, the slurry was filtered through a fritted disk, washed with six aliquots of toluene (2 cm^3), and dried under vacuum for 6 h at room temperature. The samples were labeled, combining the name of the commercial silica and the temperature employed in its pretreatment. For instance, EP 12 (250) indicated that the commercial silica from Crossfield that was pretreated at 250°C before MAO grafting.

Polymerization Reactions

Polymerization experiments were performed using 50 cm^3 of toluene in a 200 cm^3 Parr reactor connected to a constant temperature heater, with an internal temperature indicator, equipped with mechanical stirring, pressure gauge, and inlets for both argon and the monomer. MAO was used as the cocatalyst. In each experiment, the catalyst components were added in the following order: MAO, the silica support suspension, and the solution of the catalyst. Each of these components was transferred under argon. The polymerization reactions were carried out at 60°C for 30 min under 2.5 bars of ethylene. Acidified (HCl) ethanol was used to quench the process, and the reaction products were separated by filtration, washed with distilled water, and dried.

Characterization of the Supported MAO-Modified Silicas

To measure the surface areas of the supported MAO-modified silicas, samples were outgassed (10−2 mbars) at 80°C for at least 8 h. Adsorption–desorption nitrogen isotherms were measured at −196°C on a Gemini 2375 (Micromeritics, Norcross). Specific surface areas were determined by the Brunauer–Emmett–Teller equation ($P/P_0 = 0.05$–0.35) while pore volumes and diameters were determined by the Barett Joyner Halenda (BJH) method. SEM-EDX experiments were carried out on a JEOL JSM/5800. Initially, the samples were fixed on a carbon tape and coated with gold by conventional sputtering techniques. A 10 kV accelerating voltage was employed for SEM. Images were obtained using a Nanoscope III. FT-IR spectroscopy of the samples diluted in KBr was performed on pellets in transmission mode using a BOMEM FT-IR spectrophotometer (MB-102). These measurements were performed at 25°C; 32 scans at a resolution of 4 cm^{-1} were collected.

The SAXS experiments were carried out on the D2A and D11A beam lines at the Brazilian Synchrotron Light Laboratory (LNLS, Campinas, Brazil) using a wavelength $\lambda = 1.488$ nm. The X-ray beam was monochromatized with a silicon monochromator and collimated by a set of slits defining a pin-hole geometry. The incident beam was detected at two different sample-to-detector distances, 1549.8 and 2245.7 mm, to increase the scattering vector (q) range ($q = (4\pi/\lambda) \sin\theta$; 2θ = scattering angle). Dried samples were sandwiched between two Kapton® foils, and the collimated X-ray beam was passed through a chamber containing the stainless-steel sample holder. All measurements were performed at room temperature. Silver powder was used as a standard to calibrate the sample-to-detector distance, the detector tilt and the direct beam position. The transmission, dark current and Kapton™ foil corrections were performed on the 2D image before further data processing. The isotropic scattering patterns were radially averaged. Analyses of SAXS data were performed using the Irena evaluation routine implemented by the Igor Pro Software (Wave Metrics, Portland).[16] A multi-level unified fit was used to describe one or two levels of the structural organization evident in the scattering data.[17,18] In this method, the scattering provided by each structural level is the sum of a Guinier exponential form and a structurally limited power-law tail. A generalized equation, representing any number of levels, can be written as follows: [17,18]

$$I(q) = \sum_{i=1}^{n} G_i \exp\left(\frac{-q^2 R_{gi}^2}{3}\right) + B_i \exp\left(\frac{-q^2 R_{g(i+1)}^2}{3}\right) \left[\frac{\left(erf\left(qR_{gi}/\sqrt{6}\right)\right)^3}{q}\right]^{Pi}.$$

In this relation, n is the number of structural levels observed, G is the Guinier prefactor, R_g is the radius of gyration and B is a prefactor specific to the power-law scattering specified as the decay of the exponent P.

Characterization of Polymers

Polymer melting points (T_m) were determined with a DuPont DSC 2910 differential scanning calorimeter, operating in the temperature range of 25–150°C, calibrated with indium and employing a heating rate of 10°C min^{-1}. All heating cycles were performed twice. The crystallinities of the polymers were determined according to Ref. 19. Thermal gravimetric analyses (TGA) were performed with a TA Instruments SDTQ600 analyzer to evaluate interactions between the $[Al]_{MAO}$ and the studied supports. The samples (10–20 mg) were heated in the temperature range of 50–600°C under N_2. Molar masses and the molar mass distributions were determined with a Waters CV Plus 150°C high-temperature gel permeation chromatography (GPC) instrument equipped with a viscosimetric detector and three styragel HT-type columns (HT3, HT4, and HT6) with an exclusion limit of 1×10^7 for polystyrene. Analyses were performed at 140°C with the solvent 1,2,4-trichlorobenzene used at a flow rate of 1 cm^3 min^{-1}.

Table I. The Effect of Silica Calcination Temperature on the Amount of Cocatalyst Grafted and Textural Properties of Resulting MAO-Modified Silicas

Silica	Calcination temperature (°C)	Al/Si	Surface area ($m^2\ g^{-1}$)	Pore volume ($cm^3\ g^{-1}$)	Pore diameter (nm)	Surface area of the pores ($m^2\ g^{-1}$)	Total OH concentration[a]
EP12	-	-	390[b]	1.75[b]	50[b]	93[b]	-
	110	0.30	330	0.983	55	87	10.1
	250	0.23	335	0.964	60	85	5.1
	450	0.17	344	0.871	62	88	4.6
PQ	-	-	676[b]	3.07[b]	18[b]	135[b]	-
	110	0.24	561	1.03	21	96	11.3
	250	0.19	575	1.01	24	100	9.5
	450	0.27	585	0.998	40	122	8.1

RSD = 3–5%.
[a] Calculated from the area ratio between bands placed at 3460 and 798 cm^{-1}.
[b] Before calcination.

Statistical Analysis

The SPSS Statistical System (SPSS for Windows, version 19, IBM®) was used for correlation analyses.

RESULTS AND DISCUSSION

Silica is presently considered the best support for heterogenizing metallocenes. However, as-received silica contains physisorbed water, surface hydroxyl groups and siloxane groups.[20–22] The distribution of hydroxyl groups on silica surfaces may be classified by one of several descriptions: single (isolated), geminal, and hydrogen-bonded (vicinal). The calcination temperature affects the nature and the density of these surface sites, which may in turn affect the surface chemistry and the performance of the final supported catalyst. In previous work, we extensively investigated surface reactions involved either directly with the metallocene or with surface-grafted methylaluminoxane. Evidence for the type of grafting reactions taking place at the material surface and the reaction mechanism have been reported elsewhere.[13,23–26]

Scanning electron microscopy-energy dispersive X-ray analysis (SEM-EDX) is a powerful and convenient method used to determine the immobilized metal content and its distribution on the surface of the catalyst.[27,28] Table I shows the Al/Si ratio for the supported MAO-modified silicas.

According to Table I, commercial silica EP 12 has a higher Al content than PQ when calcined at 100 and 250°C. The differences in the grafted Al contents may be due to the textural differences between these two types of silica.[29] In the case of the EP 12 silica, increasing the calcination temperature results in a reduction in grafted Al content. This reduction in Al is likely due to an altered silanol density, thus providing fewer available grafting sites available for MAO.

The Al content of the support prepared from PQ MS 3065 calcined at 450°C was somewhat higher than those observed for materials calcined at 110 and 250°C. This discrepancy can be explained by the calcination-induced conversion of OH groups (geminal or isolated) into the tricyclic (three-membered) siloxane functionalities (Si—O—Si—); hence, a gradual growth of the siloxane functionality compensates for the loss of OH groups. This result indicates an increase in siloxane concentration with increasing calcination temperature led to increase Al loading. Similar behavior has been previously observed.[30,31]

The homogeneity of the distribution of the Al on the support was evaluated by SEM-EDX elemental analysis. Figure 1 show the EDX analyses of the MAO-modified support particles using the PQ and EP12 silicas pretreated at different calcination temperatures.

As shown in Figure 1, MAO is relatively well dispersed on the supports. Particularly good Al distribution was found for the PQ silica. Calcination at 110°C does not afford a homogenous distribution of Al due to relatively high OH concentrations. As will be discussed later, differences seen in the homogeneity of MAO impregnation on the various supports may contribute to the observed differences in catalyst activity.

Notably, the spherical morphology of the PQ silica is preserved after MAO modification. The specific surface area of the MAO-modified silicas calcined at different temperatures (110, 250, 450°C) was determined by nitrogen adsorption and compared with bare silica (Table I).

As shown in Table I, there are significant textural differences between the two commercial silicas. In particular, PQ possessed a much higher surface area. Thermal treatment, followed by MAO grafting, brought about a reduction in the surface areas (ca., 15%) in comparison to the value calculated for bare silica. This result suggested that MAO grafting affects the textural properties of the silica. Changes in the observed Al/Si ratio do not seem to correlate to the measured surface areas of the silica pretreated at any calcination temperature, all of which were reasonably constant.

According to Table I, a significant difference is observed in the reduction of pore volume, which ranges between 50 and 70%, in agreement with previous work.[32,33] Decreases in the pore

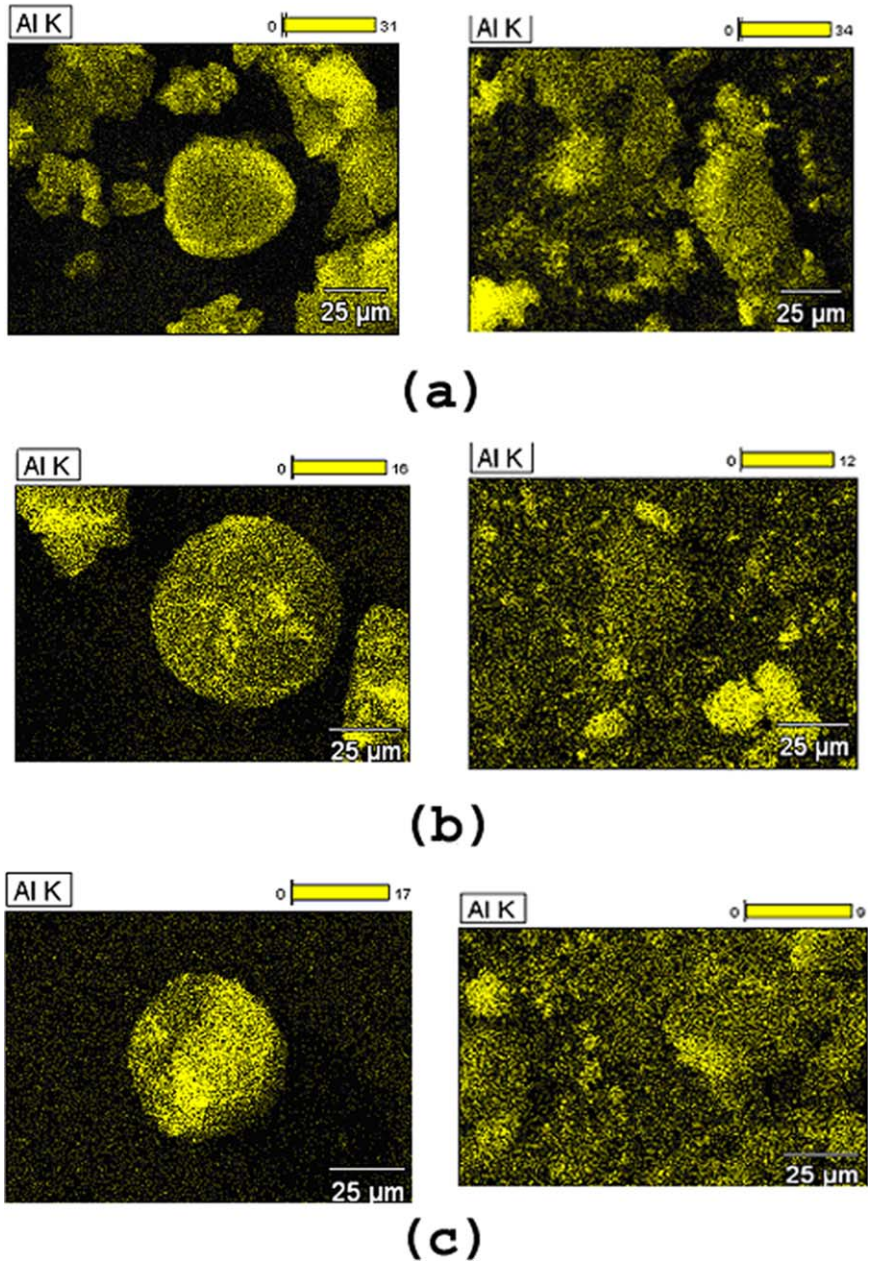

Figure 1. Al distribution on the MAO-modified PQ (left) and the EP 12 (right) silicas that were previously calcined at different temperatures: (a) 110°C; (b) 250°C: (c) 450°C. [Color figure can be viewed in the online issue, which is available at wileyonlinelibrary.com.]

volume of the silica after chemical modification show that MAO reacts with the available hydroxyl groups inside pores. Decreases in the surface area and pore diameter also confirm the successful immobilization of MAO in the supports. These results indicate that MAO grafting or impregnation likely involve sites situated within the pore network.

The availability of surface hydroxyl groups on silica can be evaluated by infrared spectroscopy (IR), and conclusions may be drawn regarding the immobilization method or the type of silica employed. Figures 2 and 3 depict the infrared spectrum of MAO modified PQ and EP12 silica at each calcination temperature. An internal reference band (750–800 cm^{-1}) was used to normalize the area of the total OH band at 3200–3500 cm^{-1} (Table I). The ratio of these areas corresponds to the total OH content on the MAO-modified silica surface. A larger number of silanol groups (available for modification) were detected in the 110°C treated MAO-modified silica compared to those prepared at 250 and 450°C. Atiqullah et al. found that commercial silicas lost all physisorbed water when heated at approximately 180°C.[31] The surface OH density in silica decreased with increasing calcination temperature. After treatment at high temperatures (450°C), the silica surface presents mainly isolated and, to a lesser extent, both geminal hydroxyl groups and surface siloxane bridges. The broad bands observed from 2600 to

Applied Polymer SCIENCE

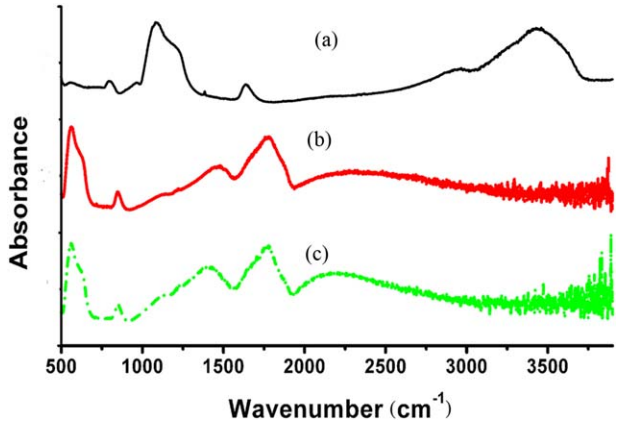

Figure 2. Comparative FT-IR spectra of the MAO modified silica PQ at different calcination temperatures: (a) 110°C; (b) 250°C and (c) 450°C. [Color figure can be viewed in the online issue, which is available at wileyonlinelibrary.com.]

3500 cm^{-1} also indicate the presence of water and a silanol species in the 110°C system.[34] The FT-IR spectrum of the silica treated at 110°C also shows a band at 1077 cm^{-1} that can be attributed to the $\nu_{as(Si—O)}$ asymmetric stretching of the siloxane rings that construct the silica network. This stretching intensity was smaller for the systems calcined at 250 and 450°C, likely due to the decrease in silanol concentration. Silicas modified at 250 and 450°C have weak intensity bands in the range of 3720–3730 and 3740–3750 cm^{-1} attributed to OH groups perturbed by hydrogen bonding and isolated surface OH groups, respectively. The latter are found as sharp bands in unmodified silica (not shown in the figures).[24]

Small angle X-ray scattering (SAXS) was used to obtain structural details about the MAO modified silica supports. Figure 4 presents the experimental SAXS data for the systems studied in this work and the unified fits for materials calcined at 110°C (other calcination temperatures showed similar particles). As no differences were observed between the scattering patterns of silicas before and after the MAO impregnation, the differences in the SAXS curves among the MAO modified silicas can be attributed to the nature of each type of commercial silica. In general, silicas are industrially produced from sodium silicate solutions; therefore, the observed differences in SAXS data may be attributed to variations in synthesis conditions such as pH, silicate concentration and drying conditions.[35]

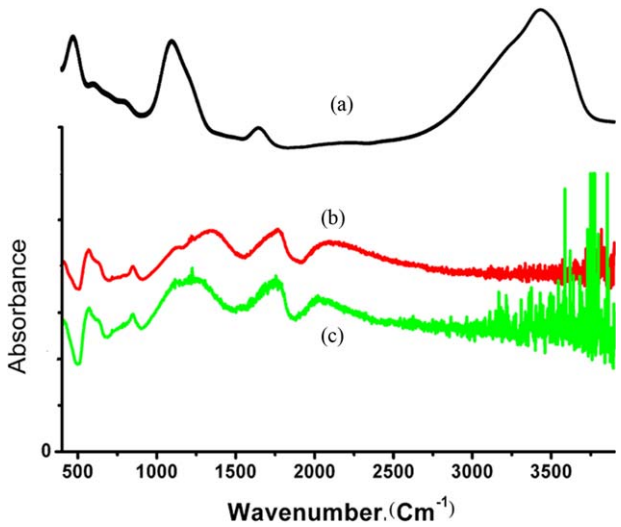

Figure 3. Comparative FT-IR spectra of the MAO modified silica EP12 at different calcination temperatures: (a) 110°C; (b) 250°C and (c) 450°C. [Color figure can be viewed in the online issue, which is available at wileyonlinelibrary.com.]

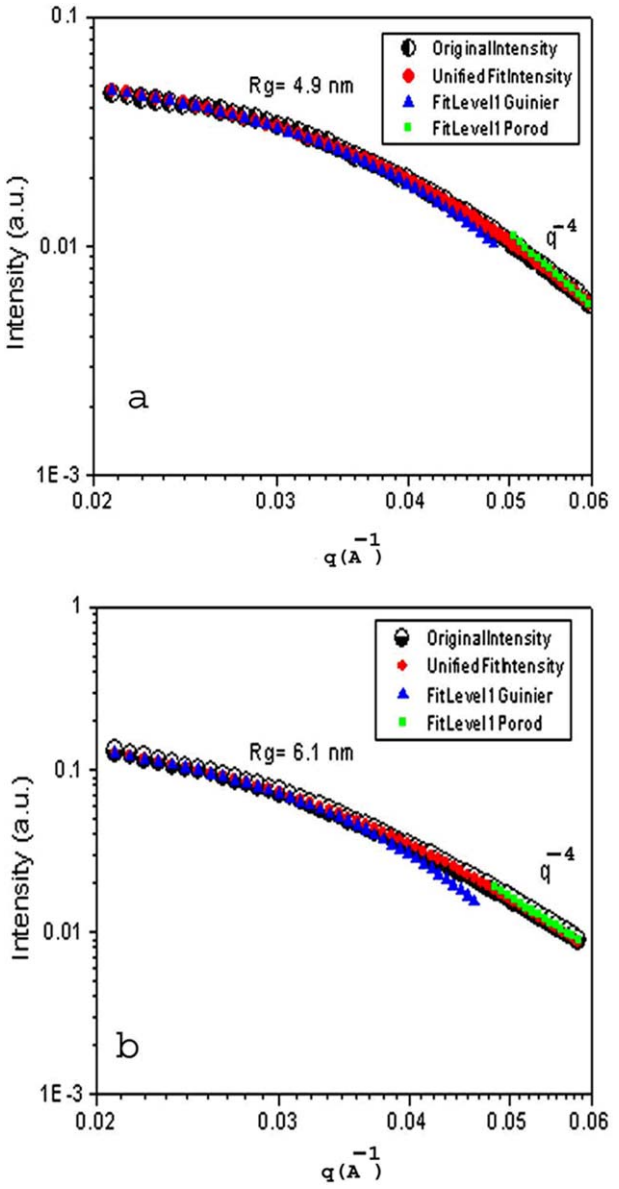

Figure 4. SAXS curves of the MAO modified silica supports calcined at 110°C (a) MAO modified silica EP12; (b) MAO modified PQ. [Color figure can be viewed in the online issue, which is available at wileyonlinelibrary.com.]

The SAXS curves of the MAO-modified silicas indicate a structure with only one level of organization containing a shoulder-type Guinier region and power-law decay. The Guinier region allows an estimation of the radius of gyration (R_g), while the

Table II. Catalyst Activity of $Et_2IndZrCl_2$ in Ethylene Polymerization Using MAO-Modified Silicas and Characteristics of the Resulting Polymers

Silica type	Al/Si	Catalyst activity (Kgpolym molZr^{-1} h^{-1})	T_m (°C)	χ (%)	M_w	M_w/M_n
Homogeneous	-	-	-	-	81,000	2.1
PQ (110)	0.24	1000	132	56	172,000	3.8
PQ (250)	0.19	800	132	57	135,000	3.1
PQ (450)	0.27	1260	132	56	n.d.	n.d.
EP12 (110)	0.3	790	131	54	152,000	4.1
EP12 (250)	0.23	610	132	56	122,000	2.9
EP 12 (450)	0.17	560	132	57	n.d.	n.d.

RSD = 5–10%.
Al/Zr = 500, [Zr] = 1×10^{-5}, time = 30 min, pressure = 2.5 bars, temperature = 60°C; χ = crystallinity.

power-law gives details about the organization of the system. According to Figure 4, the R_g values for the MAO-modified EP12 and PQ silicas were ~4.9 and ~6.1 nm, respectively, which can be attributed to the presence of elementary silica particles or the existence of pores. The latter hypothesis was disproved by N_2 adsorption–desorption analysis, which indicated pore diameters of 55 and 21 nm for the EP12 and PQ materials, respectively. These values are extremely large when compared with the SAXS measurements. The alternative scenario, in which the R_g corresponds to the elementary silica particles formed in the reaction process, is supported by earlier work.[36,37] Additionally, the power-law decay indicated that these elementary silica particles present smooth surfaces (q^{-4}). These coefficient values are related to the fractal geometry of the MAO-modified silica.

Catalysts Activity in Ethylene Polymerization

Metallocene moieties may be supported *in situ*, eliminating the necessity of a pre-polymerization supporting step, as is the case in the commercial supported MAO (SMAO). Polymerization mechanisms of such systems have been discussed elsewhere.[4,5] The in situ supported $Et[Ind]_2ZrCl_2$ is not active in the absence of trimethylaluminum (TMA)[15]; however, the addition of TMA during polymerization activated the catalyst.[4,5,14] The addition of MAO (external MAO) to the in situ supported metallocene also increases the polymerization rate.[15] The MAO-modified silica, with a low ratio of external MAO to the catalyst (Al/Zr), was used instead of commercial SMAO for *in situ* polymerization. The results of the ethylene polymerization using *rac*-$Et(Ind)_2ZrCl_2$ as the co-catalyst are summarized in Table II.

Increasing the Al/Si ratio increased the catalyst activity for both MAO modified silicas. However, as shown in Table II, increased calcination temperature for the EP 12 silica resulted in decreased catalyst activity due to a decrease in Al loading. For the MAO modified PQ silicas, the highest activity was found for the sample calcined at 450°C due to the high Al content observed by EDX (Table I). In either case, the highest activity was observed for the sample with the highest Al content. A comparison of the activities of the two series clearly indicated that the PQ silicas were more active than the EP 12 materials. The observed differences in the activities of the silica-supported catalysts may be attributed to the amounts of $[Al]_{MAO}$ present in each silica and surface properties such as the surface area and pore volume. It is worth mentioning that alkylaluminum immobilization takes place through a grafting reaction, which, in turn, depends on accessible OH groups. According to correlation analysis, in the case of EP, a strong Pearson correlation was found between the Al/Si ratio and the number of total OH groups (0.922). A strong, indirect Pearson correlation between the Al/Si ratio and pore diameter (−0.980) was also observed: the narrower the pore diameter, the higher the Al/Si content. Such results suggest that in the case of EP, a large fraction of alkylaluminum might be preferentially grafted on the uppermost surface, as achieved by low-temperature calcination (110°C). However in the case of PQ, a strong Pearson correlation was observed between Al/Si and pore diameter (0.786), suggesting that larger pore diameters are related to higher Al/Si values. It may be postulated that as thermal treatment removes the outermost silanol groups, alkylaluminum is forced to react with the remaining silanol groups available deeper within pores.

The degree of interaction between the support and the $[Al]_{MAO}$ can be determined by TGA.[38] Our study of these systems led us to propose a support-$[Al]_{MAO}$ interaction similar to those described by Pothirat et al. [39] This framework postulates that connections are formed between oxygen on the support and the Al of the co-catalyst. Because different types of support-materials have different surface properties, each may contain its own O—Al bonding scheme with different bond energies and degrees of interaction. TGA can provide useful information about the degree and strength of the $[Al]_{MAO}$ interaction with the support in terms of weight loss and the removal/decomposition temperature. Overly strong interactions between $[Al]_{MAO}$ and the support can inhibit interactions with the metallocene catalyst during the polymerization processes, leading to low polymerization activities. The TGA profiles for the $[Al]_{MAO}$ on the MAO modified silicas calcined at 110°C are shown in Figure 5 and display a similar profile for each support (similar profiles were obtained for other calcination temperatures not shown here). We observed that the weight loss of the $[Al]_{MAO}$ from each support was in the order of PQ (22%) > EP12 (13%), indicating that the $[Al]_{MAO}$ present on the EP12 support was more strongly bound than the $[Al]_{MAO}$ on the PQ support. Despite the weaker $O_{support}$–$Al_{cocatalyst}$ interactions, higher activities were obtained for the PQ support (Table II).

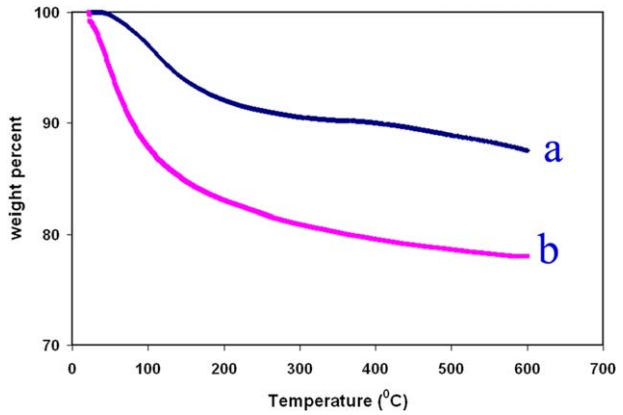

Figure 5. TGA profiles of the MAO modified supports: (a) EP 12; (b) PQ, both calcined at 110°C. [Color figure can be viewed in the online issue, which is available at wileyonlinelibrary.com.]

The resulting polymers showed similar melting points. Table II shows the molecular weight and the molecular weight distribution of the polymers produced by homogenous and supported metallocene catalysts. The molecular weight distribution of the polymers made with the *in situ* supported metallocene was broader than those made with the homogeneous catalyst. This effect may indicate that there are at least two different species active for the polymerization of ethylene on the *in situ* supported metallocene catalyst. The polymer produced with the homogeneous $Et[Ind]_2ZrCl_2$ catalyst had a narrow distribution, characteristic of a single site catalyst.

Comparison of Two Types of Silica

Table III shows a comparison between some of the properties of the two types of the MAO-modified silica. MAO modified PQ silicas showed a higher activity in polymerization than the MAO modified EP 12 silicas. This result could be explained by factors indicated in TGA and EDX analyses, including the relatively large amount of $[Al]_{MAO}$ on the PQ silica, the difference in bonding interactions between the $O_{support}$–$Al_{cocatalyst}$ on the two materials, and differences in the degrees of homogeneity of the MAO impregnation on the support surface.

Pullukat et al.[29] showed that metallocene catalysts present higher activities when supported on high-pore-volume silicas due to the resultant higher metal loading. Generally, as the pore volume increases, there is an increased tendency for the material to fragment with the accumulation of the polymer.[40] This high-pore-volume behavior was more prevalent in the MAO-modified PQ silica than in the comparatively low-pore-volume MAO-modified EP12 (Table III). The modified PQ material presented a higher surface area than the modified EP12 silica. The latter silica showed lower activity in polymerization. This result is attributed to the better accessibility of monomer units to the active sites[40] or, as suggested by Greco et al.,[41] to the presence of more evenly spaced active catalytic species. These MAO modified silicas showed somewhat higher activities than other supported systems[14,15,42] and required the addition of less external MAO ([Al] : [Zr] = 500) than other supported metallocenes, which frequently require [Al] : [Zr] = 1000–3000 to give effective concentrations of the active zirconocenium cations.[32,43,44] However, comparisons between the performances of individual catalysts should be made with caution, as polymerization conditions are seldom standardized.

Nevertheless, it is clear that the two silicas differ in terms of surface area. A multivariate analysis of MAO-modified silica characteristics, catalyst activity and polymer properties showed evidence of a strong Pearson's correlation between Al/Si ratio and catalyst activity (0.976 and 0.963 for silicas EP and PQ, respectively), indicating that such a parameter may indeed affect catalyst performance. In the case of surface area, a strong indirect Pearson's correlation was observed for the EP silica (−0.887), indicating that increasing the surface area reduces catalyst activity. For PQ silica, a modest positive correlation was observed (0.482). This result indicates the importance of silica surface area in the present results.

CONCLUSION

The activities of supported catalysts based on the two types of silica were investigated. SAXS data showed similar scattering patterns for the two the types of silica. The power-law decay indicated that the elementary silica particles present smooth surfaces. The highest activity observed for the MAO-modified silicas was achieved by material with the highest Al/Si ratio. However, the calcination temperatures of the materials yielding the best catalytic activities differed for the two types of silica (450°C for PQ and 110°C for EP12), suggesting that other textural parameters may also be responsible for the catalyst performance. The relatively higher surface area and pore volume of the PQ silica were the primary parameters affecting catalyst activity. The lower strength of the $O_{support}$–$Al_{cocatalyst}$ bond in the PQ silica, compared to that of the EP 12 material, is another reason for the higher activity. The properties of the catalytically synthesized polymers, such as the melting point and the degree of crystallinity, were not found to be dependent on the type of silica used.

Table III. Some Properties of MAO Modified Silica

MAO modified silica	Al loading	Os_{upport}–$Al_{cocatalyst}$ bonding	Pore volume	R_g (nm)	Surface area	Activity in polymerization
PQ	Higher	Weaker	Higher	6.1	Higher	Higher
EP 12	Lower	Stronger	Lower	4.9	Lower	Lower

ACKNOWLEDGMENTS

The authors thank PQ Corporation for their kind donation of silicas and LNLS for their SAXS measurements (Project SAXS1-8043). The authors also thank the Iran Polymer and Petrochemical Institute and the Ministry of Science and Technology of Iran for their support of the sabbatical financing. The authors thank also FAPERGS-PRONEX for financial support.

REFERENCES

1. Lee, H. W.; Ahn, S. H.; Park, Y. H. *J. Mol. Catal. A Chem.* **2003**, *194*, 19.
2. Severn, J. R.; Chadwick, J. C.; Duchateau, J. C. R.; Friederichs. N. *Chem. Rev.* **2005**, *105*, 4073.
3. Tullo, A. H. *Chem. Eng. News* **2010**, *88*, 10.
4. Franceschini, F. C.; Tavares, T. T.; Dos Santos, J. H. Z.; Soare, J. B. P.; Ferreira, M. L. *Polymer* **2007**, *48*, 1940.
5. Franceschini, F. C.; Tavares, T. T.; Bianchini, D.; Alves, M. C. M.; Ferreira, M. L.; Dos Santos, J. H. Z. *Appl. Polym. Sci.* **2009**, *112*, 563.
6. Tisse, V. F.; Prades, F.; Briquel, R.; Boisson, C.; McKenna, T. F. L. *Macromol. Chem. Phys.* **2010**, *211*, 991.
7. Hong, D. S.; LEE, K. S.; Cho, J. H.; Song, E. K.; Lee, Y. H.; Lee. B. R.; Kim, S. K. WO/2010/068045, **2010**.
8. Moroz, B. L.; Semikolenova, N. V.; Nosov, A. V.; Zakharov, V. A.; Nagy, S.; O'Reilly, N. J. *J. Mol. Catal. A Chem.* **1998**, *130*, 121.
9. Kim, J. D.; Soare, J. B. P.; Rempel, G. L. *Macromol. Rapid. Commun.* **1998**, *19*, 197.
10. Quijada, R. A.; Rojas, R.; Narvaez, A.; Alzamora, L.; Retuert, J.; Rabagliati, F. M. *Appl. Cata. A.* **1998**, *166*, 207.
11. Bonni, F.; Fraaije, V.; Fink, G. *J. Polym. Sci. Part A Polym. Chem.* **1995**, *33*, 2393.
12. Collins. S.; Kelly, W. M.; Holden, D. A. *Macromolecules* **1992**, *25*, 1780.
13. Dos Santos, J. H. Z.; Greco, P. P.; Stedile, F. C.; DuPont, J. *J. Mol. Catal. A Chem.* **2000**, *154*, 103.
14. Chu, K. J.; Shan, C. L. P.; Soares, J. B. P.; Penlidis, A. *Macromol. Chem. Phys.* **1999**, *200*, 2372.
15. Chu, K. J.; Shan, C. L. P.; Soares, J. B. P. Penlidi, A. *J. Polym. Sci. Part A Polym. Chem.* **2000**, *38*, 462.
16. Ilavsky, J.; Jemian, P. R. *J. Appl. Crystallogr.* **2009**, *42*, 347.
17. Beaucage, G. *Appl. Crystallogr.* **1995**, *28*, 717.
18. Beaucage, G. *Appl. Crystallogr.* **1996**, *29*, 134.
19. Mortazavi, M. M.; Arabi, H.; Zohuri, G. H.; Ahmadjo, S.; Nekoomanesh, M.; Ahmadi, M. *Macromol. React. Eng.* **2009**, *3*, 263.
20. Bortolussi, F.; Broyer, J. P.; Spitz, R., Boisson, C. *Macromol. Chem. Phys.* **2002**, *203*, 2501.
21. Ihm, S. K.; Chu, K. J.; Yim, J. H.; Soga, K.; Terano, M. Catalyst Design for Tailor-Made Polyolefins: Studies in Surface Science; Elsevier: New York, **1994**; p 299.
22. Iiskola, E. I.; Timonen, S.; Pakkanen, T. T.; Harkki, O.; Lehmus, P.; Seppala, J. V. *Macromolecules* **1997**, *30*, 2853.
23. Galland, G. B., Seferin, M., Guimarães, R., Rohrmann, J. A., Stedile, F. C., Dos Santos, J. H. Z. *J. Mol. Catal. A: Chem.* **2002**, *189*, 233.
24. Bianchini, D.; Dos Santos, J. H. Z.; Uozumib, T.; Sano, T. *J. Mol. Cat. A: Chem.* **2002**, *139*, 223.
25. Dos Santos, J. H. Z.; Ban, H. T.; Teranishi, T.; Uozumi, T.; Sano, T.; Soga, K. *Appl. Catal. A: Gen.* **2001**, *220*, 287.
26. Fisch, A. G.; Da Silveira, N.; Cardozo, N. S. M.; Secchi, A. R.; Dos Santos, J. H. Z. *J. Mol. Catal. A: Chem.* **2013**, *366*, 74.
27. Zheng, X.; Smit, M.; Chadwick, J. C.; Loos, J. *Macromolecules* **2005**, *38*, 4673.
28. Zechlin, J.; Steinmetz, B.; Tesche, B.; Fink, G. *Macromol. Chem. Phys.* **2000**, *201*, 515.
29. Pullukat, T. J.; Shinomoto, R.; Gillings, C. *Plast. Rub. Compos. Process.* **1998**, 8.
30. Wang, L.; Zhang, P. Y.; Jiang, S.; Feng, L. X. *J. Appl. Polym. Sci.* **2001**, *81*, 3186.
31. Atiqullah, M.; Akhtar, M. N.; Moman, A. A.; Abu-Raqabah, A. H.; Palackal, S. J.; Al-Muallem, H. A.; Hamed, O. M. *Appl. Catal. A Gen.* **2007**, *320*, 134.
32. Silveira. F.; Pires. G. P.; Petry. C. F.; Pozebon, D.; Stedile, F. C.; Dos Santos, J. H. Z., Rigacci, A. *J. Mol. Catal. A Chem.* **2007**, *265*, 167.
33. Smit, M.; Zheng, X.; Loos, J.; Chadwick, J. C.; Koning, C. E. *J. Polym. Sci. Part A: Polym. Chem.* **2005**, *43*, 2734.
34. Dos Santos, J. H. Z.; Krug, C.; Barbosa da Rosa, M.; Stedile, F. C.; Dupont, J.; Forte, M. D. C. *J. Mol. Catal. A Chem.* **1999**, *139*, 199.
35. Bergna, E.; Roberts, W. O. Colloidal Silica: Fundamentals and Applications, CRC Press, Boca Raton, **2006**.
36. Cardoso, M. B.; Luckarift, H. R.; Urban, V. S.; O'Neill, H.; Johnson, G. R. *Adv. Funct. Mater.* **2010**, *20*, 3031.
37. Capeletti, L. B.; Bertotto, L. F.; Dos Santos, J. H. Z.; Moncada, E.; Cardoso, M. B. *Sens. Actuators B* **2010**, *151*, 169.
38. Ketloy, C.; Jongsomjit, B.; Praserthdam, P. *Appl. Catal. A Gen.* **2007**, *327*, 270.
39. Pothirat, T.; Jongsomjit, B.; Praserthdam, P. *Catal. Commun.* **2008**, *9*, 1426.
40. Brambilla, R.; Radtkea, C.; Stedile, F. C.; Dos Santos, J. H. Z.; Miranda, M. S. L. *Appl. Catal. A Gen.* **2010**, *382*, 106.
41. Greco, P. P.; Brambilla, R.; Einloft, S.; Stedile, F. C.; Galland, G. B.; Dos Santos, J. H. Z.; Basso, N. R. *J. Mol. Catal. A Chem.* **2005**, *240*, 61.
42. Chu, K. J.; Shan, C. L. P.; Soares, J. B. P.; Penlidis, A. *J. Polym. Sci. Part A: Polym. Chem.* **2000**, *38*, 1803.
43. Lee, B. Y.; Oh, J. S. WIPO Patent WO 9,952,949, to LG Chemical Ltd, **1999**.
44. Dos Santos, J. H. Z.; Gerbase, A. E.; Rodenbusch, K. C.; Pires, G. P.; Martinelli, M.; Bichinho, K. M. *J. Mol. Catal. A Chem.* **2002**, *184*, 167.